

Thermal oxidation of tantalum films at various oxidation states from 300 to 700 °C

Ramesh Chandrasekharan

Department of Mechanical and Industrial Engineering, University of Illinois, Urbana, Illinois 61801

Inkyu Park

Department of Mechanical Engineering, University of California, Berkeley, California 94720

R. I. Masel

Department of Chemical and Biomolecular Engineering, University of Illinois, Urbana, Illinois 61801

Mark A. Shannon^{a)}

Department of Mechanical and Industrial Engineering, University of Illinois, Urbana, Illinois 61801

(Received 29 June 2005; accepted 28 October 2005; published online 12 December 2005)

This paper presents the combined use of mathematical modeling and Auger depth profiling to study and quantify the oxidation of Ta films over a wide range of temperatures. The thermal oxidation of tantalum films (~ 700 nm) is studied using direct measurements of species concentration by means of Auger depth profiling. The oxidation temperature range of this study extends from 300 to 700 °C and the oxidation period varies from 5 s to 12.5 h. The Auger depth profiles revealed that the metallic film oxidizes to first form low valence oxides of Ta that progressively convert to tantalum pentoxide with increasing temperature and time. A first-order reaction diffusion model is used to quantify the diffusion of oxygen through a film that is evolving in composition. The Auger depth profiling and reaction-diffusion model are used to estimate the actual diffusivity values for oxygen in the evolving Ta/Ta-oxide thin-film matrix, rather than more conventional techniques that estimate either the initial diffusion of oxygen through a semi-infinite metal or give a depth- and time-integrated value for the diffusivity. A comparison between the actual diffusivity values estimated in this work and the depth- and time-integrated version using the same model revealed that the integrated values are higher than the actual diffusion values by greater than 300% for the temperature range tested. Moreover, these depth- and time-integrated values for diffusivity values match over the applicable temperature ranges the diffusivity values given in the literature, which are essentially integrated average values for Ta/Ta oxide matrix. Furthermore, using the Auger depth profiles, the oxide growth rates are quantified as a function of temperature and compared with available literature. The growth rate of the oxide that is observed to be logarithmic at 300 °C is seen to have a parabolic growth at 500 °C and then a multistep growth behavior (a combination of parabolic and linear growth) at 700 °C. These growth rates and the transition from one growth type to another strongly correlate to the change in surface and film morphology and also the transition from amorphous to crystalline Ta₂O₅. © 2005 American Institute of Physics.

[DOI: [10.1063/1.2139834](https://doi.org/10.1063/1.2139834)]

I. INTRODUCTION

Tantalum pentoxide is an important dielectric material finding increasing use in capacitors, dynamic random access memories (DRAMs), optical coatings, high-temperature reflectors, antireflection coatings, etc. Most of the available literature focuses on structural and electrical properties of either bulk or very thin films of tantalum oxide.¹⁻⁴ The use of Ta and Ta₂O₅ as high-temperature reflectors in the infrared range is the motivation behind this current study. Ta itself has a very high IR reflectance ($\sim 96\%$) and Ta₂O₅ has moderately high reflectance ($\sim 50\%$), but Ta is known to oxidize readily to various oxidation states and the oxides occur in amorphous and crystalline states. Tantalum at oxidation states other than *c*-Ta₂O₅ can have much lower reflectance ($<10\%$). The oxidation and crystalline states of Ta, how-

ever, depend on the diffusion of oxygen through Ta and its various oxides as a function of temperature. Although the oxidation and crystalline states of Ta are well known, open questions remain as to what the true diffusion of oxygen is through Ta metal and oxide matrices, and whether or not the diffusion of oxygen increases or decreases due to oxidation of Ta and by how much. Thus, we conducted a study and quantification using a direct method to measure the diffusion of oxygen through Ta and its oxides. Also, given the interest in IR range reflectors, the focus is on relatively thicker films (~ 800 – 900 nm of tantalum pentoxide versus the ~ 80 – 100 nm films used in the microelectronic industry). However, the results of this current study are also applicable to thinner films.

The thermal oxidation kinetics and oxidation behavior of bulk Ta have been extensively studied⁵⁻⁸ with indirect methods that yield integrated average values for diffusion, but

^{a)}Electronic mail: mshannon@uiuc.edu

there have been fewer studies on the oxidation kinetics of thin films.⁹ Even for the oxidation of Ta thin films, the values for the diffusivity of oxygen into thin films of Ta or its oxides are presented only by Steidel and Gerstenberg.⁹ They found that the oxidation of Ta thin films differs from that of bulk Ta in many aspects. Uniform and dense Ta₂O₅ layers with an amorphous phase were produced in the oxidation of thin-film Ta, while a crystalline Ta₂O₅ layer with a nonuniform, rough surface is formed in the oxidation of bulk Ta. The oxide growth rate of Ta thin film was found to follow a parabolic behavior at temperatures between 425 and 525 °C. The authors calculate the apparent diffusion coefficient of oxygen into the Ta thin film between 250 and 375 °C using an electrical-resistance-based method to determine the formation of the oxide.

Another class of available literature presents the elemental composition variation using depth profiling techniques such as Auger electron spectroscopy or x-ray photoelectron spectroscopy (XPS) of the oxides of tantalum.^{10–12} For the studies we could find, the focus is on the initial diffusion through tantalum and does not include diffusion through films that are partially to fully oxidized. Also the values for the diffusivity of oxygen through thin films of tantalum suboxides and tantalum pentoxide were not available in the literature.

The aim of this paper is to present a more complete analysis of the thermal oxidation of sputtered tantalum films on top of Si over a wide range of temperatures of interest to microelectronics and IR reflector communities. For this, Auger depth profiling data are used to quantify the oxygen content in the film for various oxidation temperatures and durations. These values are then used in a mathematical model to compute the diffusion coefficient of oxygen through the matrix of tantalum, its oxides, and tantalum pentoxide.

II. EXPERIMENTAL PROCEDURE AND DATA REDUCTION

A. Experimental procedure

To grow the Ta thin films used in this oxidation study, metallic Ta films (0.6–0.75 μm) were deposited using dc magnetron sputtering (300 W) in an Ar atmosphere [2.5 mTorr, ~20 standard cubic centimeter per minute (SCCM)]. The sputtering substrate was a RCA SC-1-cleaned Si wafer. The Ta thin films were then oxidized in a dry O₂ atmosphere in a conventional oxidation tube furnace, where nitrogen gas was used as the inert gas before oxygen was introduced for a set time. The oxidation temperatures ranged from 300 to 700 °C and the duration of oxidation was varied from as low as 5 s to as long as 12.5 h.

The surface morphology of the films was observed using a Hitachi S-4700 field-emission electron microscope. The crystalline structure was investigated using a Philips X'Pert x-ray diffractometry system (Cu Kα radiation with λ_{rad} = 0.154 06 nm). The x-ray-diffraction (XRD) results were compared with the PCPDFWIN powder diffraction file¹³ to find the crystal plane, lattice parameter, and relevant crystal structure of the sample. The elemental compositions of the

films were measured with a Perkin-Elmer PHI-660 scanning Auger microscope, and depth profiles were obtained using an Ar ion beam *in situ* sputtering system. The 510 eV peak was used to calculate the oxygen concentration and the 179 eV peak was used for Ta (the 179 eV Ta peak was observed to shift by around 1 eV, to 180 eV or so, across the oxide/suboxide interface but the shape of the 510 eV oxygen remained unchanged as oxygen penetration proceeded). The 272 eV carbon peak was used to verify the absence of carbon contaminants in the film and to negate the possibility of charging effects (charging leads to a shift of the C peak from 272 eV). The raw data were converted to the correct compositions by the use of a standard Ta₂O₅ sample.

B. Using AES results to estimate sputter depth and oxide thickness

The composition of the thin films was investigated using Auger elemental surface analysis and Ar ion sputtered bombardment to mill down in depth. The Auger electron spectroscopy (AES) depth profiles presented in Fig. 1 were originally obtained as plots of the elemental composition as a function of the Auger Ar gun sputter time. The sputter time is converted into a sputter depth by measuring the sputter rate for both Ta₂O₅ and Ta. A Dektak-3 profilometer gave a sputter rate of 47 nm/min for tantalum oxide and 62 nm/min for Ta. The sputter rate used depends on the oxygen concentration, with a mixture rule assumed between the Ta₂O₅ and Ta rates to determine the final depth.

The interface between the Ta₂O₅ layer and the underlying tantalum suboxide layer is not sharp, which complicates the estimation of the oxide thickness. Since Ta has many oxidation states, the point where the Ta can be assumed to be fully coordinated with oxygen as an oxide and where oxygen exists interstitially within a Ta metal matrix is somewhat arbitrary. Thus, the oxide thickness d is estimated to be the depth where the oxygen concentration is equal to the mean of the oxygen concentration within the tantalum pentoxide layer and the oxygen concentration within tantalum suboxide layer as shown in Fig. 2. Thus, d is estimated to be the point where

$$C_{\text{oxygen}}(d) = 0.5[C_{\text{oxygen}}(\text{Ta}_2\text{O}_5 \text{ layer}) + C_{\text{oxygen}}(\text{suboxide layer})]. \quad (1)$$

C. Data reduction methods for diffusion analysis

The initial thermal oxidation of pure Ta can be viewed as the interstitial dissolving of oxygen into a Ta matrix that then leads to a saturated matrix, which is followed by oxide formation. The sequential nature of these processes is explained in detail by Pozdeev-Freeman *et al.*¹¹ The diffusion of oxygen occurs without noticeable reaction until the saturation of the Ta matrix occurs. Hence, we employ a simple diffusion model to quantify the initial oxidation of Ta and to determine the diffusion coefficient when oxygen concentration in Ta is very low. However, on saturation, the diffusion occurs in tandem with the reaction of oxygen with tantalum. Thus, the effect of the reaction of oxygen with Ta creates an additional

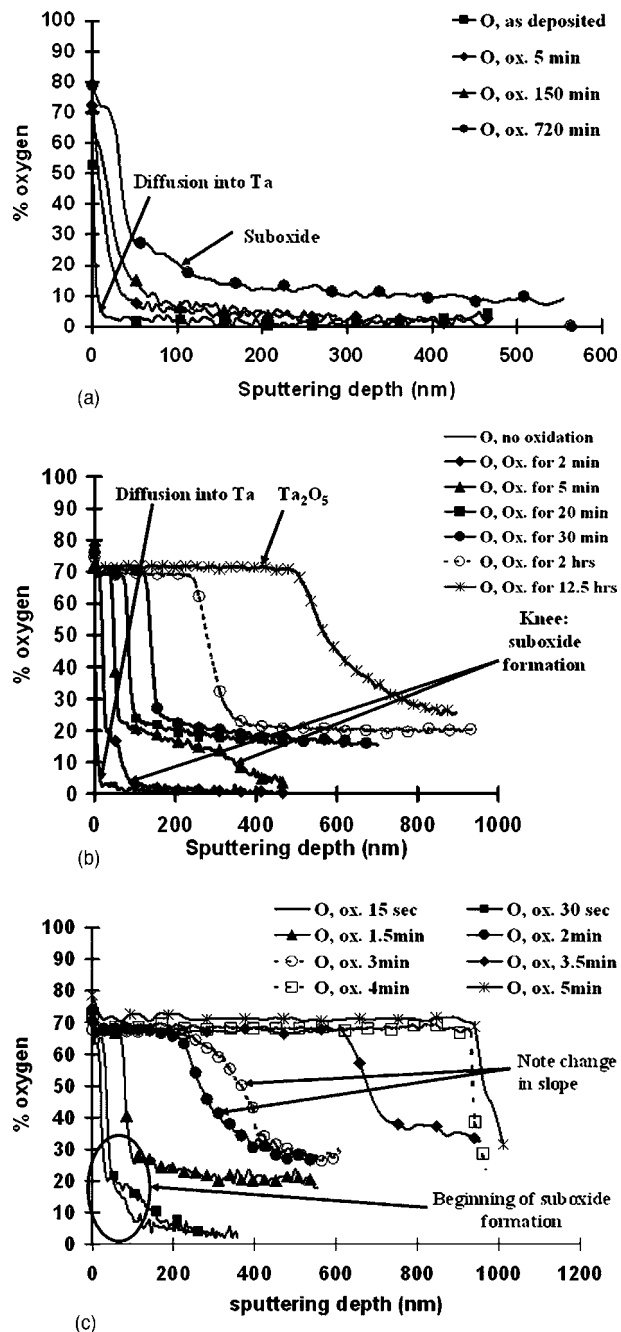


FIG. 1. AES depth profile of Ta thin films heated in oxygen at 300, 500, and 700 °C. The depth profiles show the oxygen concentration as a function of the depth from the surface of the thin film. In (a), note that the initial oxidation profiles (oxidation times <5 min) show oxygen concentrations approaching zero in the bulk of the Ta film. Also, note that the oxygen concentration for the entire film increases with temperature, but is below the 71.4% oxygen concentration of Ta_2O_5 , save for an ~10 nm layer at the surface for 720 min of oxidation. The formation of a stoichiometric pentoxide at the top of the film is seen only after the film first forms suboxides. In (b), compared to (a), note the formation of pentoxide at the surface of the film after 2 min of oxidation, which grows thicker as the oxidation period increases. The formation of the suboxides occurs where “knees” in the oxygen concentration profile are seen. The overall oxidation process at 500 °C, however, is essentially similar to 300 °C, where the metallic film first gets converted to a suboxide and only then to a stoichiometric oxide at the surface. In (c), note that the oxide layer is formed after just 5 s of oxidation (as compared to the 2+ min for oxidation at 500 °C). The presence of the knees in the oxygen concentration profiles are more pronounced than in the 500 C oxidation profiles. The fundamental difference of the oxidation profiles for 700 °C from the other profiles is the change in the slope of the profile after 3 min of oxidation due to crystallization.

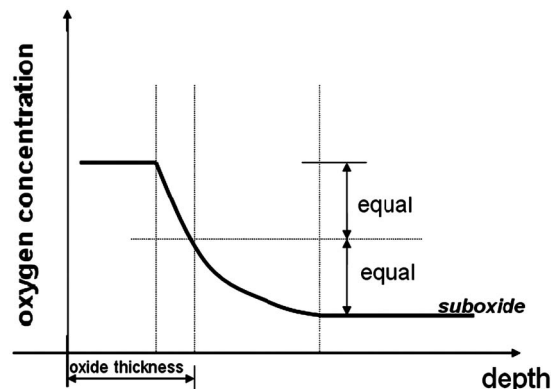


FIG. 2. The method used to estimate the oxide thickness. The thickness is the depth where the oxygen concentration is equal to the mean of the oxygen concentration within Ta_2O_5 layer and the oxygen concentration within tantalum suboxide layer.

impedance on the transport of oxygen diffusing through the film that needs to be accounted for in the model. Therefore, we employ a reaction-diffusion model to quantify the oxidation of Ta and tantalum oxide and to determine the diffusion coefficients at higher oxygen concentrations.

In the available literature, most estimates of the diffusion coefficients use indirect techniques via resistance measurements, gravimetric studies, etc., to determine changes in oxygen concentration over time at given temperatures. When these techniques are applied to the thermal oxidation of Ta, an integrated average diffusion coefficient over time and distance (depth of the film) results, where the oxygen varies from interstitial to saturation concentrations and where tantalum oxides are formed. The values obtained for the diffusivity in this current study are spatially and temporally defined, to clearly delineate the diffusion into Ta, suboxides, and amorphous and crystalline tantalum pentoxides. To compare these results with those in the literature, we also present an integrated analysis that uses the reaction-diffusion model developed here to estimate the apparent diffusivity, which is the actual quantity that is typically reported in the literature.

1. Diffusion from ambient oxygen flow into the Ta film

The initial oxidation of Ta is modeled as the diffusion of oxygen into a semi-infinite matrix of Ta. The semi-infinite assumption is supported at early times in Figs. 1(a)–1(c) when the oxygen concentration goes to zero with penetration well before the thickness L of the Ta film is reached. The surface boundary is assumed to be at a constant concentration of oxygen for the atmospheric pressure used (based on evidence from Refs. 6, 9, and 14). Assuming a homogeneous and isotropic diffusion coefficient D , the transient one-dimensional mass diffusion equations are given as

$$D \frac{\partial^2 C}{\partial x^2} = \frac{\partial C}{\partial t}, \quad (2)$$

$$C(0, t) = C_0, \quad (3)$$

$$C(x,0) = C_i, \quad (4)$$

where C is the concentration of oxygen, C_0 is the concentration of oxygen at the surface of the Ta, C_i denotes the initial concentration of oxygen within the Ta, and x denotes the depth from the surface. The nondimensional solution to these equations is

$$\frac{C(x,t) - C_0}{C_i - C_0} = \operatorname{erf}\left(\frac{x}{2\sqrt{Dt}}\right). \quad (5)$$

The unknown parameters C_0 and diffusivity D are found using a nonlinear least-squares solver based on the Gauss-Newton/Levenberg-Marquardt method to fit Eq. (5) to the Auger depth profile at the initial oxidation stage. The assumption of a semi-infinite Ta was checked once the calculations for diffusivity were completed and was found to be valid, where $2\sqrt{Dt} \ll L$.

2. Reaction-diffusion analysis

The reaction-diffusion mechanism is employed to model the transport of oxygen through a matrix of oxides of tantalum at various valence states. Tantalum is able to coordinate with 1–7 oxygen atoms and readily coordinates with oxygen up to 5 oxygen atoms. Thus, we include in the transient diffusion model a reaction-rate term that has a first-order dependence on the local concentration of oxygen, such that

$$D \frac{\partial^2 C}{\partial x^2} - kC = \frac{\partial C}{\partial t}, \quad (6)$$

$$C(0,t) = C_0, \quad (7)$$

$$C(x,0) = C_i, \quad (8)$$

where C is the concentration of oxygen, C_0 is the concentration of oxygen at the surface of the Ta film, C_i denotes the initial concentration of oxygen within the Ta film, k denotes the rate of reaction of the solute (oxygen), and x denotes the depth from the surface. The reaction diffusion model in Eq. (6) (Ref. 15) allows for some of the oxygen to be bound and immobilized into the matrix, for reactions that are of first order for the reaction of oxygen with Ta. For spontaneous coordination to oxygen, this assumption is reasonable. Hence this method estimates the oxygen that is moving through an oxygen-concentration-dependent matrix, as opposed to the oxygen that is bound with Ta. The movement of oxygen through the tantalum oxide matrix is not likely freely diffusing, rather more of a lattice hopping mechanism. However, since the transport of an atom via lattice hopping is favored in the direction of lower concentration, the resulting transport essentially behaves like pure diffusion, and can be modeled as such.

The nondimensional solution to the reaction-diffusion equations (6)–(8) is

$$\begin{aligned} \frac{C(x,t) - C_i}{C_0 - C_i} = & \frac{1}{2} \exp\left(-x \sqrt{\frac{k}{D}}\right) \operatorname{erfc}\left(\frac{x}{2\sqrt{Dt}} - \sqrt{kt}\right) \\ & + \frac{1}{2} \exp\left(x \sqrt{\frac{k}{D}}\right) \operatorname{erfc}\left(\frac{x}{2\sqrt{Dt}} + \sqrt{kt}\right). \end{aligned} \quad (9)$$

Similar to the prior case, the diffusivity is found using a least-squares error analysis. The variables are grouped together in order to reduce the number of parameters in the curve fit for the unknowns C_0 , k , and D . Hence, the following equation is used to find the parameters using the Gauss-Newton/Levenberg-Marquardt method:

$$\begin{aligned} C(x,t) - C_i = & \frac{1}{2} \exp(a - bx) \operatorname{erfc}(cx - d) \\ & + \frac{1}{2} \exp(a + bx) \operatorname{erfc}(cx + d), \end{aligned} \quad (10)$$

where a is $\ln(C_0 - C_i)$, b is $\sqrt{k/D}$, c is $1/(2\sqrt{Dt})$, and d is \sqrt{kt} .

3. Estimation of an integrated diffusion coefficient from the Auger analysis

Next, the integrated diffusion coefficient, over time and depth, is estimated for oxygen diffusing into the Ta-oxide matrix. The basic premise used is that all the oxygen present in the initially metallic Ta film has entered through the surface. Thus, the total molar flux of oxygen at the surface, j_0 , over the oxidation time equals the total number of moles of oxygen in the film, such that for the one-dimensional (1D) geometry

$$\int_0^{t_{\text{oxidation}}} j_0 dt = \int_0^{\infty} C dx. \quad (11)$$

The integral on the right-hand side is determined experimentally by measuring the total area under the curve for a given concentration depth profile measured as a function of the distance from the surface. Using

$$j_0 = -D_{\text{O-Ta}} \frac{\partial C_0}{\partial x} \quad (12)$$

and Eq. (9), the integrated diffusion coefficient for oxygen into Ta is

$$\begin{aligned} D_{\text{int}} \left\{ \int_0^{t_{\text{oxidation}}} \left[\sqrt{\frac{k}{D}} \operatorname{erfc}(-\sqrt{kt}) - \sqrt{\frac{k}{D}} \operatorname{erfc}(\sqrt{kt}) \right. \right. \\ \left. \left. + \frac{2}{\sqrt{\pi Dt}} e^{-kt} \right] dt \right\} = \frac{2}{(C_0 - C_i)} \left(\int_0^{\infty} C dx \right), \end{aligned} \quad (13)$$

where D_{int} is the depth- and time-integrated value of the actual diffusivity. To evaluate the above integral, the value of k , $C_0 - C_i$, and the spatially dependent D is obtained from the curve-fitting routine using Eq. (10).

III. SUMMARY OF DIFFUSION COEFFICIENT RESULTS

The diffusivity of oxygen into a Ta metal matrix is calculated using the curve-fitting routine using Eq. (5) for the

TABLE I. Summary of oxidation rates and diffusivity for various oxidation temperatures.

$T_{\text{oxidation}}$ (°C)	Oxide layer growth	Oxide layer growth kinetics (d : nm, t : min)	$D_{\text{O-Ta}}$ (initial oxidation) [m ² /s] ($\times 10^{-18}$)]	$D_{\text{O-Ta/oxide matrix}}$ [m ² /s] ($\times 10^{-18}$)]	k [s ⁻¹] ($\times 10^{-3}$)]	Nature of the oxide
300	Logarithmic	$d = B_1 \log(t+1)$ $B_1 = 4.7923$	3.4 (± 0.9)	7.7 (± 0.7)	7.2	Amorphous suboxides, thin
500	Parabolic	$d = B_2 t^{1/2}$ $B_2 = 21.517$	48 (± 7)	2.6 (± 0.5)	7.3	amorphous Ta ₂ O ₅
700	Parabolic+linear	$d = B_2 t^{1/2}$ ($t < 1.5$) $B_2 = 64.36$ $d = B_2(t-1.5)^{1/2} + B_3$ ($1.5 < t < 3$) $B_2 = 249.26$ $B_3 = 84.6$ $d = B_4(t-3) + B_5$ ($3 < t < 4$) $B_4 = 577.16$ $B_5 = 371.3$	1200 (± 400)	106 (± 10)	110	Amorphous suboxides and Ta ₂ O ₅ Poly-crystalline Ta ₂ O ₅
300–700	Mixture of growth types	Temperature dependence $D(T) = D_0 \exp(-E_a/RT)$	D_0 (m ² /s) 5.7×10^{-15}	E_a (J/mol) 36.9×10^3	7.2–110	Ranges from metal to pentoxide

initial oxidation curve in Figs. 1(a)–1(c). The diffusivity through the Ta-oxide matrix is calculated for all the noninitial oxidation curves using the curve-fitting routine and Eq. (10). Both these values along with the value of the parameter k from Eqs. (9) and (13) are presented for three different temperatures, 300, 500, and 700 °C in Table I. The values presented in Table I for diffusion into the Ta/Ta-oxide matrix are the expected values at the respective temperatures calculated for four or five different oxidation times. The value for the diffusion into Ta metal is based on the initial oxidation curve. Figure 1 will be fully discussed in the next section.

In the literature, the temperature dependence of the diffusion coefficient is usually given by an Arrhenius form such as

$$D(T) = D_0 \exp\left(-\frac{E_a}{RT}\right), \quad (14)$$

where $D(T)$ the diffusion coefficient at absolute temperature T , D_0 is the preexponential factor, E_a is the activation energy, and R is the ideal gas constant (8.314 J/mol K). To determine D_0 and E_a , the values for $D_{\text{O-Ta}}$ and $D_{\text{O-Ta/oxide matrix}}$ are found using all the data gathered from Fig. 1 and are fitted to the data using a linear regression of $\ln(D)$ vs $1/T$. For the data presented in Fig. 1, $D_0 = 5.7 \times 10^{-15}$ ($\pm 1.4 \times 10^{-15}$) m²/s and $E_a = 36.9$ (± 7.8) kJ/mol using the data from the reaction diffusion analysis. Note that these values are weighted more by oxygen diffusing through the Ta/oxide matrix at later times, since the data collected at the three temperatures range from 5 s to 12.5 h. Higher temperatures and later times produce oxides, as shown in Fig. 1, which typically have a lower diffusivity than the metal matrix, as seen in Table I. Thus these temperature-dependent coeffi-

cients are likely smaller than if through a purely metal Ta matrix.

Finally, the significance of the parameter k is noted. Low values of k signify a lower coordination between the oxygen present in the film and Ta. There is a one-one correspondence between the value of k and the difference between the diffusivity values of oxygen calculated by Eqs. (5) and (10). Higher coordination (implying high levels of oxidation) occurs at higher temperatures and the use of Eq. (5), which is the more commonly used method to estimate the diffusivity, will lead to a significant error in estimating the diffusivity.

Figure 3(a) compares the integrated average diffusion coefficient results determined in this study with those in the literature cited here. The values calculated in this study are quite similar to those of the bulk Ta study by Powers and Doyle¹⁶ for the temperature range over which they conducted the study (150–200 °C). Similarly, the values presented by Steidel and Gerstenberg⁹ for thin films of Ta are quite similar to the integrated values from this study for the temperature range over which they present diffusivity values (200–300 °C). However, the diffusivities calculated in this study using either the reaction-diffusion model or its integrated form do not match with the extrapolated predictions of the values available in literature.^{9,10,16}

Furthermore, a comparison of the diffusion coefficients presented by Giber and Oechsner¹⁰ for oxygen through Ta and Ta₂O₅ shows that the effect of oxidation reduces the diffusion of oxygen into the film by 1–3 orders of magnitude, depending on the temperature. At low temperatures, when the film is more of a Ta metal than an oxide matrix, the integrated values D_{int} calculated in this study closely match the values for diffusivity presented by Steidel and

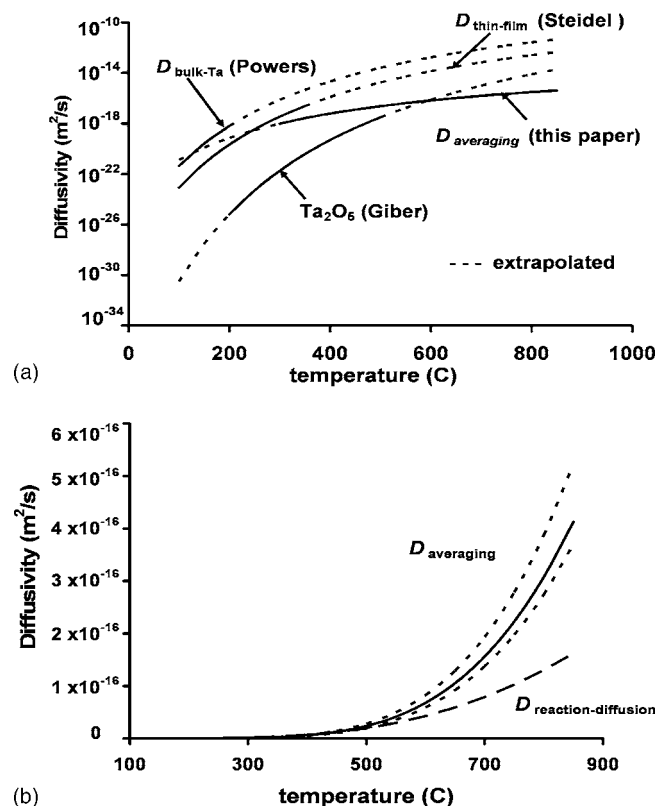


FIG. 3. In (a) the diffusivity values calculated in this study using an averaging of the reaction-diffusion model with the diffusivity of oxygen into Ta and Ta₂O₅ are compared to those available in the literature. The plots also include extrapolated values for both the current study and the diffusivity values in the literature (the extrapolation was done assuming an Arrhenius dependence on temperature). Note that the integrated diffusivity values calculated in this study are approximately equal to the diffusivity values calculated for thin films by Steidel and Gerstenberg for temperatures up to 300 °C. For higher temperatures, the integrated diffusivity values of this study are closer to the diffusivity reported for stoichiometric tantalum pentoxide by Giber *et al.* In (b), the diffusion coefficient of oxygen into Ta and its oxides is plotted using the integrated technique and the reaction-diffusion method. Note that the reaction-diffusion values are representative of the instantaneous oxygen diffusion rates than the integrated values and are much lower than the integrated version of the reaction-diffusion model.

Gerstenberg,⁹ Powers and Doyle,¹⁶ and Giber and Oechsner¹⁰ for Ta. However, as the temperature increases, the integrated values approach that for the diffusivity of oxygen through Ta₂O₅ presented by Giber and Oechsner.¹⁰ In fact, the integrated value for the diffusivity calculated in this study at 600 °C matches with that predicted for Ta₂O₅ by Giber and Oechsner,¹⁰ which is the temperature at which the film is converted into amorphous tantalum pentoxide.

IV. DISCUSSION OF OXIDATION OF TANTALUM FILMS

The oxidation behavior of Ta films on Si substrate is discussed for three different temperatures (300, 500, and 700 °C). Figure 1 captures the oxidation behavior at these temperatures. Applying the mathematical techniques presented in Sec. II to the AES profiles, the diffusion and subsequent formation of oxide were calculated. The expected diffusivity and reaction-rate values for the three different temperatures as determined by the reaction-diffusion model are presented in Table I, and the oxide growth rate is summarized in Fig. 4 and in Table I.

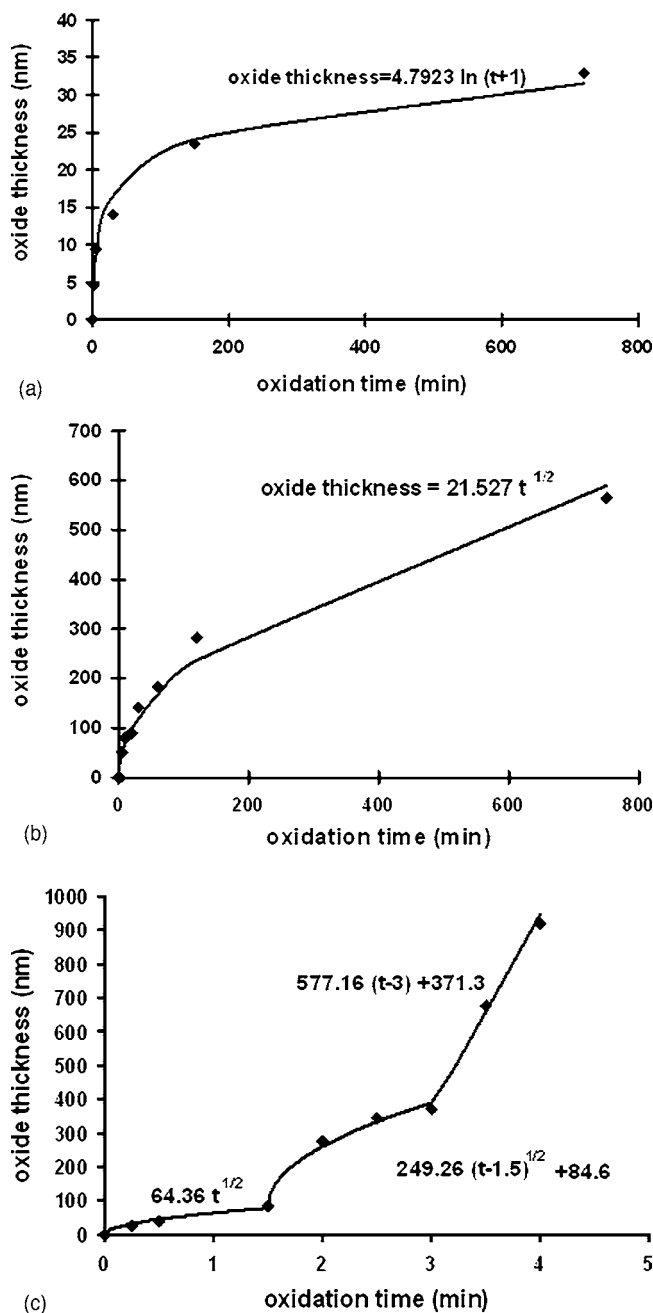
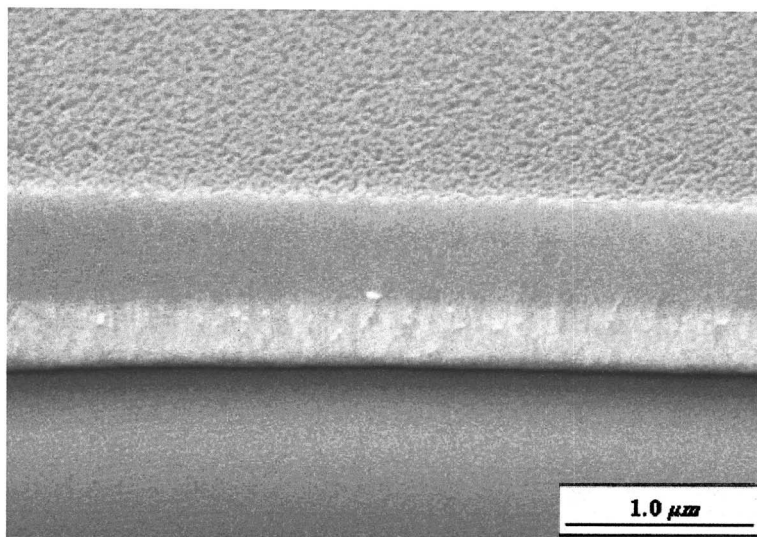
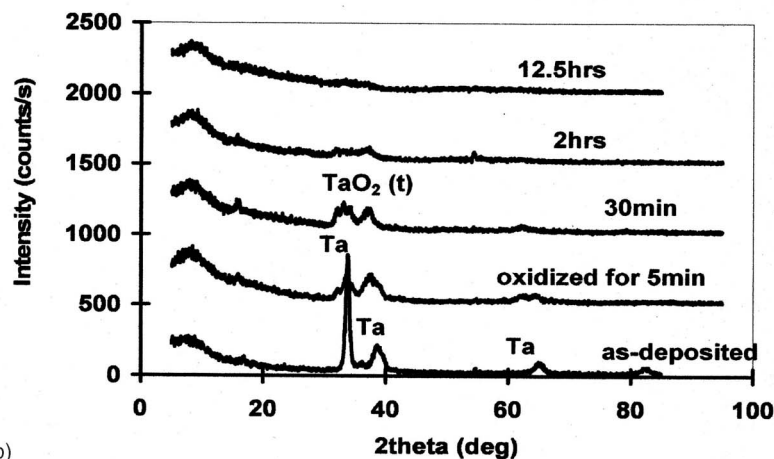


FIG. 4. The oxide thickness of Ta thin films oxidized in dry O₂ at atmospheric pressure is plotted as a function of time at three different temperatures. (a) The logarithmic oxide layer growth at 300 °C is shown. The oxide thickness follows a logarithmic function $d=B_1 \ln(t+1)$ (d : oxide thickness in nanometers t : oxidation time in minutes), where $B_1=4.7923$. (b) The parabolic oxide growth rate at 500 °C is shown. The oxide thickness follows a parabolic function of $d=B_2 t^{1/2}$ (d : oxide thickness in nanometers, t : oxidation time in minutes), where $B_2=21.527$. (c) The multistep oxide growth is shown at 700 °C with the first and the second step as parabolic and the final as linear growth rate. The oxide thicknesses are $d=B_1 t^{1/2}$ ($t < 1/5$ min), $d=B_2(t-1.5)^{1/2}+B_3(1.5 < t < 3$ min), and $d=B_4(t-3)+B_5$ ($3 < t < 4$ min) (d : oxide thickness in nanometers, t : oxidation time in minutes), where $B_1=64.36$, $B_2=249.26$, $B_3=84.6$, $B_4=577.16$, and $B_5=371.3$.

In Fig. 1(a), it is seen that the observed mechanism is one of the oxygen diffusing through the Ta film and filling up the interstitial spaces, or oxygen dissolving into Ta. The initial oxygen concentration curves for small periods of oxidation show little oxide formation. Only after the entire Ta matrix is saturated (more than 3% oxygen in the matrix¹¹)



(a)



(b)

FIG. 5. Surface morphology and crystalline structure of tantalum oxide formed by thermal oxidation of Ta thin film at 500 °C. (a) Cross-section view of Ta thin film after oxidation for 12.5 h. The oxidized Ta thin film consists of a tantalum pentoxide layer, a tantalum suboxide layer, and a silicon substrate from surface top to the bottom. It was observed that the tantalum pentoxide formed as a uniform and dense layer. (b) Evolution of crystalline structure of oxidized Ta thin film. After 2 h of oxidation, crystalline peaks of Ta disappear and no peaks are observed after 12.5 h of oxidation, indicating that the resulting tantalum oxide is amorphous.

does oxide formation begin in the film, which is signified by the formation of a “knee” in the graphs in Fig. 1. On saturation of the Ta thin film with oxygen, diffusion of oxygen continues through the Ta–O matrix, along with the formation of tantalum pentoxide at the top of the film and tantalum suboxides in the bulk of the film. The diffusion thus changes from one where oxygen diffuses into a Ta metal matrix to one where oxygen diffuses through a matrix of Ta metal and its suboxides. This change in the nature of diffusion is seen for all the three temperatures presented. The only difference is the period of time that the Ta film remains metallic in character. For 300 °C, the suboxide formation is not seen until after 5 min of oxidation. For greater periods of oxidation, the thickness of the oxide formed at the surface is limited. For 500 °C, the time for which diffusion can be thought of as occurring into Ta is less than 2 min, and it is less than 15 s for oxidation at 700 °C.

The rate of oxide growth at any temperature is depen-

dent on many factors including the diffusion of oxygen into the film and the reaction of oxygen with the metal and suboxides. The diffusivity of oxygen at various temperatures was presented in the previous section and showed an almost Arrhenius dependence on the temperature [Eq. (14)]. The values of the parameter k (which quantifies the reaction rate for the coordination between oxygen and Ta) obtained by the curve-fitting analysis are presented in Table I. The values, as expected, are very low for 300 and 500 °C and show a marked increase for 700 °C. The change in oxide growth rate with increasing temperature depends on the reactivity and diffusivity of the matrix with temperature, as well as the morphology of the film as will be discussed later.

At 300 °C, the oxide layer thickness growth is logarithmic [Fig. 4(a)], while it is parabolic at 500 °C [Fig. 4(b)]. At these temperatures, the oxides formed are amorphous [as shown by Fig. 5(b)] and the oxygen has to diffuse through this amorphous tantalum pentoxide layer in order to react

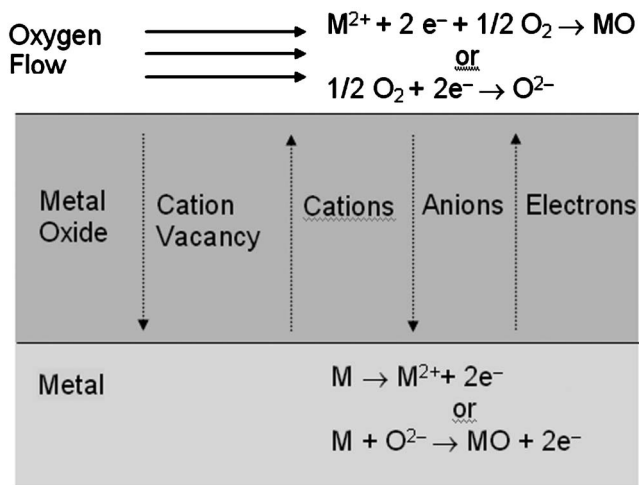


FIG. 6. Schematic model of diffusion-controlled parabolic oxidation in Wagner's theory. The oxidation rate is governed by the transport of reacting ions or electrons across the oxide scale.

with the underlying metal and suboxide to form additional tantalum pentoxide. Thus it is expected that the oxide growth rate profile should follow the oxygen diffusion profiles. Furthermore, from Table I, the value of k for 300 °C is lower than the values at higher temperatures. This lower value for k signifies a smaller reaction rate for the coordination between oxygen and Ta and points to the process being primarily diffusive.

At 300 °C the AES profiles nearly fit a complementary error function. Such profiles are expected for diffusion of one species into a semi-infinite matrix. Thus, the oxide growth is expected to be logarithmic with time, which is indeed the case. Similar logarithmic growth rates have been reported in the literature for semi-infinite media.^{5,16} For example, Vermilyea⁵ and Kofstad⁶ found that the oxide growth rate follows either an inverse logarithmic law given by $1/d = k_1 - k_2 \log t$ or a direct logarithmic rate law given by $d = k_1 \log t + k_2$.

At 500 °C, the oxide growth rate is parabolic. The slopes of the AES profiles in Fig. 1(b) are less steep than those in Fig. 1(a) for oxidation at 300 °C. However, the direction of the slope still indicates a transport-limited phenomena, wherein the diffusing oxygen has to pass through the amorphous oxide and then diffuse into the suboxides. Such a transport-limited process is expected to be parabolic for finite domains. Wagner modeled oxidation rates governed by the transport of reacting ions or electrons through the compact oxide scale.¹⁷ Wagner proposed that the initial oxidation is by the transport of cation M^{2+} as shown in Fig. 6.

The oxidation rate

$$R(t) = \frac{dX}{dt} = \text{const } j_{M^{2+}}, \quad (15)$$

where X is the oxide layer thickness, t is the oxidation time, and $j_{M^{2+}}$ is the cation flux. The cation flux $j_{M^{2+}}$ is equal and opposite of the flux of cation vacancies from the oxygen flow to the metal layer. Thus,

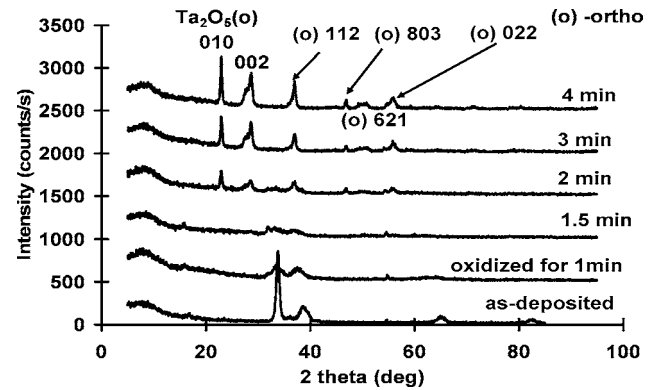


FIG. 7. XRD pattern of Ta thin film oxidized at 700 °C. The peaks of crystalline Ta_2O_5 are not observed until after 1.5 min of oxidation, indicating an amorphous phase of Ta_2O_5 . Between 1.5 and 2 min of oxidation, a crystalline phase of Ta_2O_5 begins to appear. The peaks of crystalline Ta_2O_5 increase as the oxidation period increases, indicating increasing amounts of crystal formation.

$$j_{M^{2+}} = -j_{V_M} = D_{V_M} \frac{C''_{V_M} - C'_{V_M}}{x}, \quad (16)$$

where D_{V_M} is the diffusion coefficient for cation vacancies and C''_{V_M} and C'_{V_M} are the concentrations of vacancies at oxide-oxygen and oxide-metal interfaces, respectively. If one assumes a thermodynamic equilibrium at both interfaces, the value of $(C''_{V_M} - C'_{V_M})$ is a constant leading to

$$R(t) = \frac{dx}{dt} = \text{const } j_{M^{2+}} = \text{const } D_{V_M} \frac{C''_{V_M} - C'_{V_M}}{x} = \frac{k'}{x}, \quad (17)$$

where $k' = \text{const } D_{V_M} (C''_{V_M} - C'_{V_M})$ is a constant. An integration of this gives a parabolic rate equation,

$$x^2 = 2k't + k_2. \quad (18)$$

Thus, Wagner's model that assumes a transport-limited behavior is able to predict the parabolic rate of growth we observed at 500 °C. It must be noted that the overall nature of oxidation at 300 and 500 °C is similar; the only difference is the larger thickness of oxide formed at the top at 500 °C. Also, this parabolic behavior agrees with prior studies of the oxidation of bulk Ta in the 450–600 °C temperature range reported by Kofstad⁷ for bulk tantalum and by Steidel and Gerstenberg⁹ for thin films of tantalum.

The oxide formed at 700 °C is crystalline when oxidized for more than 2 min (Fig. 7). The crystalline nature of the oxide leads to changes in the surface morphology and the oxide growth (Fig. 8). The polycrystalline nature of the oxide combined with volumetric and thermal stresses leads to cracks and pores for oxidation periods greater than 3 min [Fig. 8(b)]. The change from the amorphous to crystalline matrix structure increases the rate of diffusion through the oxide, which can also be seen in the change in slope after 2 min of oxidation in Fig. 1(c). The increase in diffusion before cracking is presumably due to the formation of grain boundaries, which provide regions of lower atomic packing density. Figures 4(c) and 7 show that the oxide growth rate changes from a slower to a faster parabolic rate at the onset

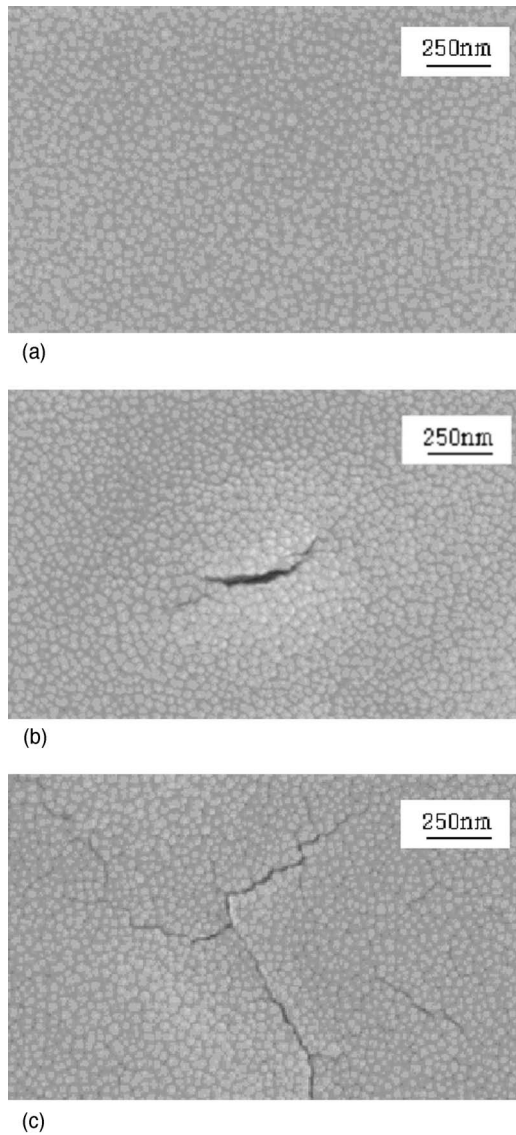


FIG. 8. Evolution of surface morphology caused by thermal oxidation at 700 °C. (a) At 1 min of oxidation, a change of surface morphology is not observed. (b) At 3 min of oxidation, the surface becomes rough and small cracks begin to appear while large oxide grains are formed. (c) At 4 min of oxidation, the surface becomes even rougher and more cracks are observed while more large grains are formed.

of crystallization. Once cracks, pinholes, and pores form, the oxygen has multiple paths to travel through the film. Apart from the usual diffusion through the oxide that forms on the surface of the film, the oxygen permeates through the cracks and pores, thereby increasing the observed oxidation rate. As soon as crystallization occurs (2–3 min of oxidation, as seen from the XRD in Fig. 7), the slope of the oxygen diffusion profiles in Fig. 1(c) shows a change in sign (second derivative goes from positive to negative—change in profile is pointed out in the figure). Furthermore, from Fig. 4(c), after 3 min of oxidation, the oxide layer growth is observed to be linear. The linear nature of oxide growth is because of the zero-order dependence on diffusion that occurs as a result of the cracks and pores. Such a linear behavior has been reported by Kofstad⁸ for bulk Ta. The authors cited in this

paper do not report on the initial oxidation growth rates and hence the initial parabolic growth could not be compared with the literature cited here.

V. CONCLUSION

Tantalum thin films thermally oxidize to form suboxides of tantalum pentoxide, Ta₂O₅. Auger spectroscopic profiles reveal the sequential nature of the oxidation process: the metal film first saturates with oxygen, converts to a suboxide, which then progressively becomes richer in oxygen until Ta₂O₅ is formed. The time required for each of these steps decreases with increasing temperature. The time required for the saturation and conversion of the film to nonpentoxide suboxides is relatively short (<15 s at 700 °C and <5 min at 300 °C) compared to the time required to convert the film into Ta₂O₅. Thus, the diffusion of oxygen into the film cannot be viewed as a process of diffusion into metal or diffusion into tantalum pentoxide. The oxygen diffuses into a variable oxide matrix with a continuously changing oxygen concentration. This process is modeled as a reaction-diffusion process to provide numerical values for the diffusivity of oxygen into the oxidizing tantalum film. The adoption of a reaction-diffusion model helps to account for the fact that the oxygen measured by AES at any depth of the film could be either bound as an oxide or could be oxygen diffusing into the film.

The adoption of the reaction-diffusion model to calculate the diffusivities is different from the approach used in the literature, where the apparent diffusivities are measured in a spatially integrated and time-integrated sense. Comparing the values of the diffusivities obtained by the reaction-diffusion model with the values calculated by a time- and depth-integrated analysis on the oxygen concentration profiles reveals that the apparent integrated diffusivity of oxygen into the Ta oxide matrix is larger than the actual diffusivity by up to greater than 300%. Thus the values reported for the diffusivity in the literature that are based on integrated analyses are higher than the actual diffusivity values.

Also, with an increase in temperature of oxidation, the increased diffusion rates are found to be directly related to the change of the film from amorphous to crystalline form. Further increases in diffusion rates for prolonged exposure at higher temperatures are found to be the result of extrinsic defects from pinholes, pores, and cracks in the films.

ACKNOWLEDGMENTS

The authors are grateful to Dr. Mauro Sardela and Nancy Finnegan for their assistance in the use of x-ray diffractometry and Auger electron spectroscopy. The experimental work in this paper was carried out in the Center for Microanalysis of Materials, University of Illinois, which is partially supported by the U.S. Department of Energy under Grant No. DEFG02-91-ER45439). This work has also been supported by Department of Defense Multidisciplinary University Research Initiative (MURI) program under Grant No. DAAD19-01-1-0582 and *The Water CAMPWS*, a Science and Technology Center under National Science Foundation Agreement No. CTS-0120978.

- ¹E. Atanassova and D. Spassov, *Microelectron. Reliab.* **38**, 827 (1998).
- ²G. Eftekhari, *Phys. Status Solidi A* **146**, 867 (1994).
- ³E. Atanassova, D. Spassov, A. Paskaleva, J. Koprinarova, and M. Georgieva, *Microelectron. J.* **33**, 907 (2002).
- ⁴S. W. Park and H. B. Im, *Thin Solid Films* **207**, 258 (1992).
- ⁵D. A. Vermilyea, *Acta Metall.* **6**, 166 (1958).
- ⁶P. A. Kofstad, *J. Inst. Met.* **91**, 209 (1962).
- ⁷P. A. Kofstad, *J. Inst. Met.* **90**, 253 (1961).
- ⁸P. A. Kofstad, *J. Electrochem. Soc.* **110**, 491 (1963).
- ⁹C. A. Steidel and D. Gerstenberg, *J. Appl. Phys.* **40**, 3828 (1969).
- ¹⁰J. Giber and H. Oechsner, *Thin Solid Films* **131**, 279 (1985).
- ¹¹Yu. Pozdeev-Freeman, A. Gladkikh, M. Karpovski, and A. Palevski, *J. Electron. Mater.* **27**, 1034 (1998).
- ¹²NIST α -ray photoelectron spectroscopy database V. 3.3, web version—<http://srdata.nist.gov/xps/>
- ¹³Powder diffraction file, CD-Rom: PCPDFWIN, version 2.0, International Center for Diffraction Data, Newtown Square PA, USA, 1998.
- ¹⁴A. G. Gusakov, S. A. Raspopov, A. A. Vecher, and A. G. Voropayev, *J. Alloys Compd.* **201**, 66 (1993).
- ¹⁵J. Crank, *The Mathematics of Diffusion*, 1st ed. (Oxford University Press, Oxford, 1967).
- ¹⁶R. W. Powers and M. V. Doyle, *J. Appl. Phys.* **30**, 514 (1959).
- ¹⁷C. Wagner, *Z. Phys. Chem.* **21**, 25 (1933).